Geomorphology 123 (2010) 330–342

Contents lists available at ScienceDirect

Geomorphology

journal homepage: www.elsevier.com/locate/geomorph

OSL-based lateral progradation and aeolian sediment accumulation rates for the Apalachicola Barrier Island Complex, North Gulf of Mexico, Florida

W.J. Rink *, G.I. López

School of Geography and Earth Sciences, McMaster University, 1280 Main St. W. Hamilton, Ontario, Canada L8S 4K1

ARTICLE INFO

Article history:
Received 9 March 2009
Received in revised form 15 July 2010
Accepted 1 August 2010
Available online 6 August 2010

Keywords:
Quartz
Optically stimulated luminescence (OSL)
Beach ridge
Geochronology
Aeolian sedimentation rate
Progradation rate

ABSTRACT

Vertical sediment cores in five separate beach ridge complexes along the north-east Gulf of Mexico Coast were recovered and dated using optically stimulated luminescence (OSL) dating of quartz: these are located on Cape San Blas (CSB), Little St. George Island (LSGI), Richardson's Hammock (RH), St. Joseph Peninsula (SJP) and Saint Vincent Island (SVI). All of these landforms are coastal barrier systems situated along a 100 km stretch of the Florida Panhandle, U.S.A. Two samples were collected for dating from each core. Ridge accumulation rates (RAR) associated with lateral progradation were calculated from the dated samples. We also determined average sediment accumulation rates (ASAR) for two intervals within each sediment core. All OSL ages within the sediment cores were found to be in stratigraphic order or in a few cases statistically indistinguishable. Moreover, all dated ridges were found to be in correct temporal sequence based on their geomorphic positions. Rapidly accreted sequences were found to be backed by St. Joseph Bay in the western region of the study area. More slowly accreted sequences were associated with the more eastern stretches of the study area backed by St. Vincent Sound and Apalachicola Bay. Our ASAR results are in accord with an Australian study of modern dune accumulation. Perhaps our most important finding is that in the barrier island environments of this north-eastern Gulf Coast region, aeolian sedimentation continues well after full vegetative cover develops and stranding of landward ridges takes place. This confirms our similar earlier observation on SVI (López and Rink, 2008). We find that up to approximately one order of magnitude lower sedimentation rates occur after an initial period of more rapid aeolian accumulation for the vertical intervals studied in foredune ridges. Lateral progradation rates of ridge sequences were highly variable within the study area, ranging from 92 to 848 m/100 years, but we did find agreement between some of our slower ridge accumulation rates and those in other areas of Florida and around the world determined using OSL and ^{14}C dating. We conclude that OSL may be used in a regional context to establish variation in progradation rates and aeolian accumulation that varies among systems.

1. Introduction

Progradational barriers or strandplain complexes (Clifton and Hunter, 1982) are characterized by multiple, coast-parallel beach or foredune ridges (Roy et al., 1994). The genesis of these landforms has been discussed by Davies (1957), Bird (1976), and Hesp (1984), among others. Sandy beach ridges are formed by the interaction of a multitude of factors throughout their time of development. They are relict coastal ridges that may form in various ways such as a combination of water- and wind-deposited material (cf. Otvos, 2000), continual accumulation of wind-blown sand over a pre-existing foredune/backshore with active vegetation growth (cf. Hesp, 1984), swash-built ridges (cf. Tanner, 1995) or welded-ridges over pre-existing foredunes, such as swash-berms built during high tides, storms and/or hurricanes (cf. Otvos, 2000; Rink and Pieper, 2001). The construction of beach ridges around the world depend on the local characteristics of the surrounding coastal environment/basin, as some formation mechanisms may have been more relevant than others during their development. In essence, beach ridges are relict coastal landforms, isolated from current shore processes (cf. Otvos, 2000) that may control the progradation of a coastal area, provided that enough sediment is supplied and that preservation happens through time (cf. Taylor and Stone, 1996).

A more recent redefinition of sand beach ridges has been attempted by Hesp (2006) which clearly separates them from foredune ridges. Beach ridges were redefined as swash-aligned, swash and storm wave built deposits or ridges formed primarily by sand, pebbles, cobbles (gravel) or boulders, or a combination of these. Hesp (2006) specifies that these are purely or principally marine deposits formed by wave action. In contrast, Hesp (2006) reiterates that foredunes are genetically and morphodynamically distinct from beach ridges, being typically the foremost vegetated sand dune formed on the backshore zone of beaches

* Corresponding author.
E-mail address: rinkwj@mcmaster.ca (W.J. Rink).

0169-555X/$ – see front matter © 2010 Elsevier B.V. All rights reserved.
doi:10.1016/j.geomorph.2010.08.001

by aeolian deposition. They are further characterized as generally shore-parallel, vegetated, ramps, terraces and convex ridges separated by concave swells (c.f. Hesp, 1999). In sandy ridge environments, foredune ridge accretion rates are relatively high as the incipient foredune progresses into an established dune, as the system accretes seaward and the ridge grows vertically (Hesp, 2002).

With the advent of optically stimulated luminescence (OSL) dating of sediments in 1985, a new approach to dating the progradation of barriers became available that greatly augments use of ^{14}C approaches. However, not until the development of the single aliquot regeneration dose protocol (SAR; Murray and Wintle, 2000) for OSL has the method begun to be used for more applications and gain general acceptance by coastal scientists. Fundamental work on the natural light exposure of sediments found in the nearshore and in a hurricane built-berm by Rink and Pieper (2001) and Rink (2003) showed that quartz in sands collected in swash, storm berms and surf zone (water depths up to 1 m) had fully zeroed OSL signals. Though these studies were mainly focused on the possibility of using the slow decay of thermoluminescence (TL) signals to study sand transport, the OSL component of the study yielded important results for OSL dating of sediments along coastlines: the likelihood that sands sourced from these zones along the coast would have fully zeroed OSL signals at the time they later became part of prograding ridge sequences (aeolian or marine). This is the fundamental condition needed for reliable OSL age determinations.

Previous quartz SAR-OSL dating for reconstruction of the timing of clastic-rich coastal sedimentary ridge sequences only started about 6–8 years ago. Ballarini et al. (2003) obtained SAR-OSL chronologies of <10 to a few hundred years old, allowing them to evaluate the evolution of a barrier island off the coast of the northern Netherlands, which were in excellent agreement with well-known historical evidence. In a different study, Banerjee et al. (2003) demonstrated the efficacy of SAR-OSL dating of stranded dune ridge sequences spanning over the past 250,000 years in the Coorong Coastal Plain, South Australia. The goal of these two studies was not to obtain coastal progradation rates but rather to prove the validity, precision and accuracy of OSL dating in both young and old clastic-rich coastal environments.

Quantification of coastal progradation rates on barrier islands and beach/dune ridge systems using OSL has been done in a number of studies. Murray-Wallace et al. (2002) demonstrated a relatively rapid but variable relict foredune development and beach ridge strandplain progradation over the past 6000 years for Guichen Bay, South Australia. According to their OSL ages and despite the multiple occurrences of truncated relict foredunes, a linear progradation rate of 0.39 m/year was obtained for the younger region of strandplain, the past 4000 years, yielding a progradation rate of one foredune every 80 years. Recent work in Florida (Rink and Forrest, 2005) focused on an extensive sequence of relict beach ridges on Cape Canaveral, Florida. They used OSL to determine a progradation rate of 135 ± 12 m/100 years. OSL chronologies were also used to determine progradation rates in raised strandplain sequences formed along Lakes Michigan and Superior, in the Upper Peninsula of Michigan, USA. Argylan et al. (2005) obtained variable progradation rates for lake-derived ridge sequences. For the past 1500 years, one ridge was forming every 28 to 50 years roughly, depending on the strandplain location. Between 1500 and 2000 years ago, the rates are quite variable, with one ridge forming for every 62 to 137 years, depending on the strandplain location. Attempting to understand the time of initiation and formation (i.e. sediment budget) of coastal dunes throughout the Skallingen Spit, Denmark, Aagaard et al. (2007) used OSL-dating and obtained new indications for the origin of coastal dune initiation after the Little Ice Age. Their OSL ages were in correct agreement with cartographic evidence and other independent dating techniques. The average vertical accretion rates obtained at three sites ranged from 0.13 to 0.18 m/year.

Earlier work on rates of progradation of coastal barriers has been carried out in using ^{14}C dating of enclosed shell materials. One example is the early work in six sites along the south-eastern coast of Australia in a variety of Holocene coastal environments (Thom et al., 1978; Chapman et al., 1982). The average rates of barrier progradation ranged from 24 m/100 years to 57 m/100 years. In this early work, radiocarbon dating on shell fragments was used, notwithstanding the problems of mixing discussed by Roy (1991). As such, other works using this technique are not elaborated here due to the problem of retention of old shell fragments that can make the ages too old.

The aim of our paper is 1) to calculate progradation rates and ridge accumulation rates (RAR) using OSL for some barrier systems within the Apalachicola Barrier Island Complex; and 2) to determine the vertical average sediment accumulation rates (ASAR) within individual sediment cores, and compare them among ridges with a view toward variation with distance from the modern shoreline.

2. Study area

The Apalachicola Barrier Island Complex (ABIC) is located along the North Florida Gulf of Mexico shoreline both east and west of the town of Apalachicola. Our study area is mainly west of Apalachicola. The Apalachicola River, which is the largest river in Florida, empties into the Gulf at this point. ABIC is a series of sand bodies comprised mainly of barrier islands that form over 100 km of coastline extending from the Ocklocknee River Mouth in the east (84° 20′ west longitude) to the entrance to St. Joseph Bay in the west (85° 25′ west longitude). Fig. 1 shows the study area, which is the westernmost portion of this complex. North–south trending St. Joseph Peninsula (SJP) lies on the west edge; Cape San Blas (CSB) at its southwestern edge; Saint Vincent Island (SVI) is further east and Little St. George Island (LSGI) is at the lower right, our easternmost segment. More than 60% of this coastline is pristine and unpopulated, protected as parts of a National Wildlife Refuges (SVI), a state park (Northern SJP), or state-owned lands (LSGI). Only the southern portion of St. Joseph Peninsula and the eastern ¾ of the bight extending from CSB, at the southern end of SJP, through to the Indian Peninsula, at Indian Pass, are occupied by residential homes.

The ABIC provides a range of well protected and developed beach ridge sequences, some of which have formed predominantly continuous, longitudinally dominant strandplains (i.e. SVI, LSGI and CSB) and others elongated, laterally accreted spits (i.e. SJP) (see Fig. 1). It presents a diverse set of natural coastline orientations resulting from different hydrodynamic conditions. This has led to a varied array of ridge trends and accretionary sequences deposited during the Late Holocene.

In our study area, there are foredune systems that are forming along all the modern shorelines. For the sand ridges that are located further inland there are strandplain ridge features that are capped by aeolian sediments. The genesis of these inland sand ridges may either be strictly by progressive stranding of previously established foredune ridges formed on back beaches by vegetative capture of sand, or by aeolian deposition on top of swash-built beach ridges. We cannot establish clearly which of these is the case for each because our cores have not penetrated deeply enough. Even though we have no strong evidence for marine sediments in the form of shells within our sediment cores, some of the sedimentary features such as horizontal to near-horizontal laminations near their bases might be related to swash-built structures, probably a product of marine influence. However, as the evidence is inconclusive, we generally view the dated upper intervals to be mainly associated with aeolian deposition.

2.1. Previous studies on the evolution and geochronology of the Apalachicola Barrier Island Complex

Previous studies related to the morphological evolution of the ABIC date back to 1961, when the first attempts to understand this area were based on studies of the former Apalachicola Delta (Tanner, 1961). The majority of these studies have been related to sedimentology, mineralogy, geomorphology, archaeology, and sea-level histories. Several attempts at

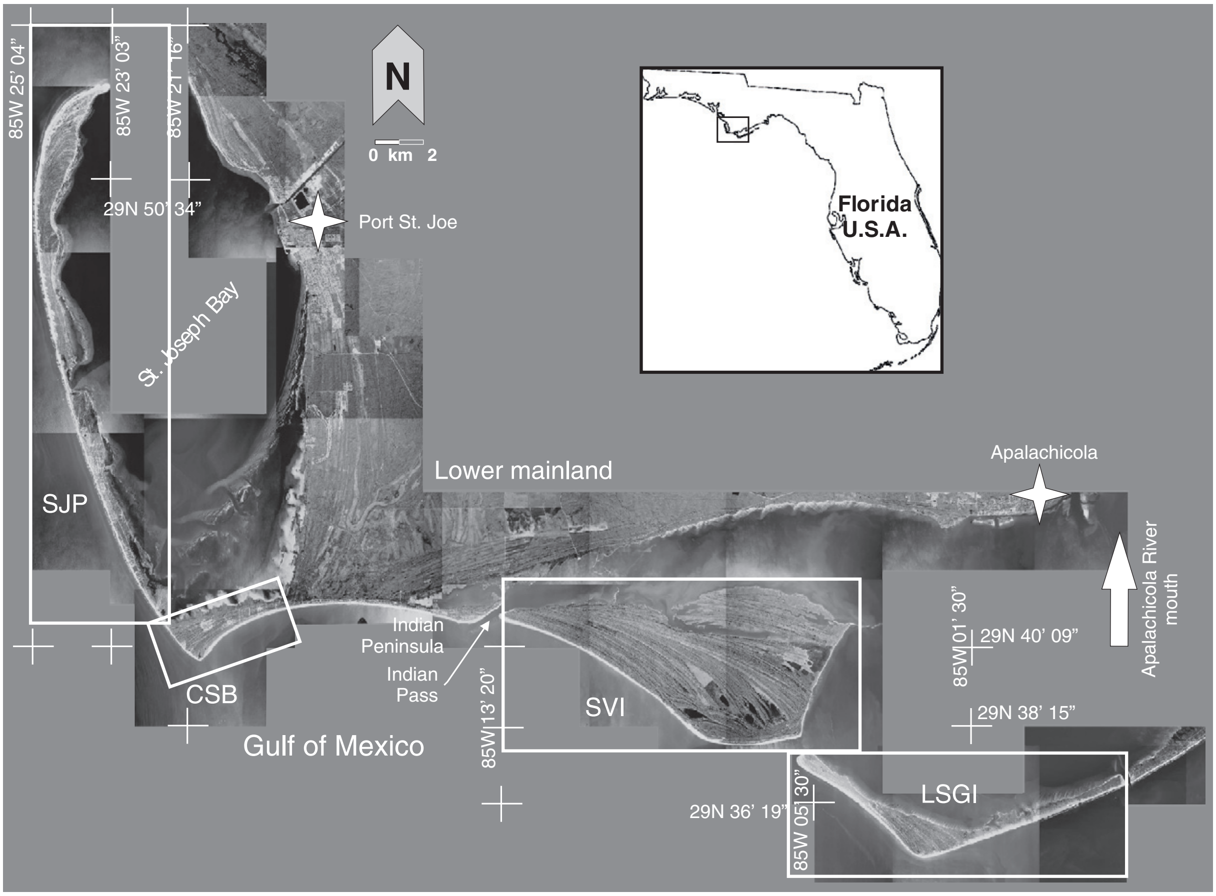

Fig. 1. Study area showing St. Joseph Peninsula, Richardson's Hammock, Cape San Blas, St. Vincent Island and Little St. George Island, within the Apalachicola Barrier Island Complex, northeastern Gulf of Mexico. The rectangles correspond to the subsequent Figs. (2)–(5) for each barrier system analyzed herein. Images from DOQQ (USGS, 1999); geographical coordinates in NAD 83.

the understanding of both the formation and evolution of the Complex as a whole and/or as individual barriers have also been made (e.g. Stapor, 1975; Rizk, 1991; Otvos, 1992).

Stapor (1973, 1975) was the first to report an evolutionary model for the formation of SJP (Fig. 2) and CSB (Fig. 3). In his model, the initial growth of the SJP was related to the formation of barrier islands which later served as nuclei in its evolution. According to his work, the first nuclei to form were Richardson's Hammock and the area just north of Eagle Harbor, and later in Holocene history, they connected by longshore drift accretion. A single radiocarbon date of 750 ^{14}C-years B.P. was associated with Stapor's work; a peat collected from near the south end of Richardson's Hammock.

In general, Stapor's model was accepted by Rizk (1991). The latter divided SJP into 14 ridge sets based on individual ridge morphological characteristics such as orientation, curvature and truncation. He explains the supra-tidal progradation and general evolution of the peninsula based on these assigned ridge sets.

More recently, Otvos (2005) reported four TL ages along the peninsula ranging from 1000 to 1700 years ago, one on Richardson's Hammock of 2900 years ago, and two on CSB of 600 and 900 years ago. From these and other considerations, he generally concurred with Stapor's original model.

Recently published dissertations have also provided dating evidence in our study area. Forrest (2003) obtained four OSL ages on SJP, all in good concordance with the present study, ranging from 8 to 1800 years ago. López (2007) provided the foundation of the work in the study presented here.

The beach ridges in the strandplain on SVI (Fig. 4) were first divided into "Pattern Sets" by Stapor (1973, 1975). Later, they were subdivided into "Ridge Sets" based on geomorphology, sedimentology and elevation characteristics by Stapor and Tanner (1977) and Tanner (1992). The geochronology of SVI began with radiocarbon dating by Stapor (1975) who obtained an age of 2110 ± 130 ^{14}C-years B.P. on *Mulinia sp.* found on the coastline in a shell bed about 3 km south of the north-eastern corner of the island. On the central northern coastline at Paradise Point, Miller et al. (1981) reported a radiocarbon age on a charcoal lens of 1710 ^{14}C-years B.P. Otvos (2005) reported 15 OSL ages and two TL ages in eight ridges throughout the island. They ranged from −6 ± 3 to 6930 ± 790 years ago. His oldest ages are generally discordant with our findings. Most recently, López and Rink (2008) reported OSL ages in from both the south-western and north-eastern ridge sequences that ranged from 370 ± 50 to 2860 ± 340 years ago.

To our knowledge, neither previous subdivisions of the ridge patterns on LSGI (Fig. 5), nor any geochronological work has been reported. Its central portion is characterized by a sandy ridge sequence forming a strandplain, while the eastern and western portions are narrower sand spit features.

3. Sampling and methodology

Long vertical and short horizontal sediment cores were taken throughout the ABIC at various locales as shown in Figs. 2–5. The sediment cores were collected with a portable gas-operated vibra-core at the crest or on the middle of the slope of the selected ridges. Samples from cores were selected based on visual observations of homogeneity of the sediment in order to insure uniform gamma irradiation. The uppermost sample was collected at a burial depth of at least 50 cm below the surface while the lowermost sample was collected as deep as

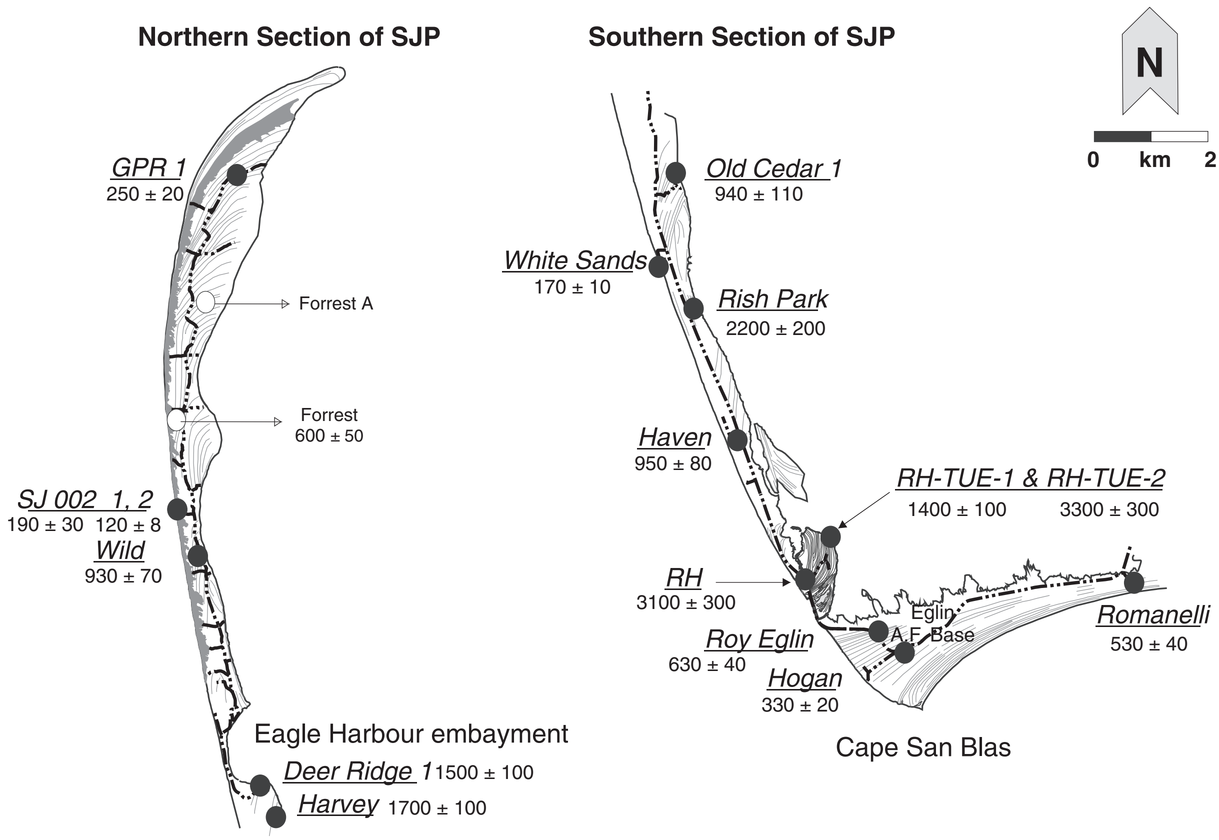

Fig. 2. Geomorphological map of St. Joseph Peninsula, Richardson's Hammock and Cape San Blas showing the location of the sediment cores collected. OSL ages given (in years before *datum*) correspond to the lowermost sample of each sediment core. The Forrest sample, with an OSL age of 600 ± 50 years, is from Forrest (2003). Location Forrest A is its counterpart traced northward along the same ridge that was used to calculate RAR values with respect to GPR 1. Beach ridges, blow-outs and washover areas are also shown. Barrier system and geomorphological attributes traced and compared from DOQQ images from USGS (1999, 2004) and topographic/bathymetric 7.5 Minute Series Orthophotomaps "St. Joseph Point Quadrangle, Florida Gulf CO — 29085-G4-TB-024", "St. Joseph Peninsula Quadrangle, Florida Gulf CO — 29084-F4-TB-024" and "Cape San Blas Quadrangle, Florida Gulf CO — 29085-F3-TB-024", USGS (1982). Geographical coordinates are in NAD 83. For symbols refer to the legend in Fig. 3.

possible into the sediment core, avoiding the areas near the core catcher that could have been potentially perturbed during the coring process.

Coarse-grain quartz separates (i.e. 150–212 μm) were obtained after preparing each OSL sample under subdued orange lighting following standard laboratory protocols (i.e. chemical and mechanical treatments) highlighted in López (2007) and López and Rink (2008).

Prior to the measurement of each sample's final equivalent dose (D_E) used in the determination of the age of each individual sample, a series of luminescence tests were performed on several single aliquots of each sample to determine the following (see López, 2007; López and Rink, 2008 for details): a) Initial assessment of the D_E value; b) Infrared test to check any contamination by feldspars; c) Pre-heat Plateau test; d) Dose Recovery test; and e) Thermal Transfer test. The final D_E was measured using the single aliquot regenerative (SAR) protocol (Murray and Wintle, 2000) at two different aliquot sizes (8 and 3 mm mask sizes) on 18 to 48 aliquots per sample. The reported OSL ages are from the 8 mm mask size D_Es, and the 3 mm measurements were used as comparisons to these to check for incomplete zeroing.

All measurements were done using an automated RISØ TL-DA-15 reader with blue light-emitting diodes (emission centered at 470 ± 30 nm) for OSL stimulation (at 125 °C for 100 s), which was measured through a 6 mm-thick Hoya U-340 filter. An infrared laser diode unit (emission centered at 830 ± 30 nm) was used for infrared stimulation. The first 0.4 s of the stimulation were used as the OSL signal, whereas the average value of 10 channels in the last 4 s was subtracted as background.

The D_E of each sample was obtained from calculating the average of the D_E values obtained from each aliquot measured. Most samples did contain one aliquot (out of 24 or 48) with a value greater than $+2\sigma$ of the mean in the D_E distribution. The D_E mean was then recalculated excluding this single value; however, no statistically significant difference was seen in the mean D_E after the removal of this outlier. The calculated D_E error of each sample corresponds to one standard deviation of the D_E values used from the distribution.

Once the ages were obtained, vertical accretion rates were calculated for individual cores containing two samples (i.e. lower sample A and upper sample B). All cores were corrected for compaction which was assumed linear throughout the sediment core. The average sediment accumulation rate (ASAR), which is an estimate of the amount of the average rate of vertical sediment deposition that occurred over specific depth intervals, was calculated for two portions of each core (and sites) using the SAR-OSL ages as follows:

$$Lower\,ASAR = (A\,vs.\,B\,depth\,difference)\,/\,(A\,vs.\,B\,age\,difference)$$

$$Upper\,ASAR = (Ground\,surface\,vs.\,B\,depth\,difference)\,/\,(Ground\,surface[age = 0]\,vs.\,B\,age\,difference)$$

Ridge accumulation rates were calculated for some beach ridge sequences, provided that these contained sufficient samples. Digital Orthoquad images — DOQQ — from available years (e.g. USGS, 1999, 2004) and topographic/bathymetric orthophotomaps (e.g. USGS, 1981, 1982) of the study area were analyzed in detail and combined with field reconnaissance to produce the maps shown in Figs. 1–5. Ridge counts were obtained from the DOQQs and orthophotomaps, and were constrained by visual inspection in the field.

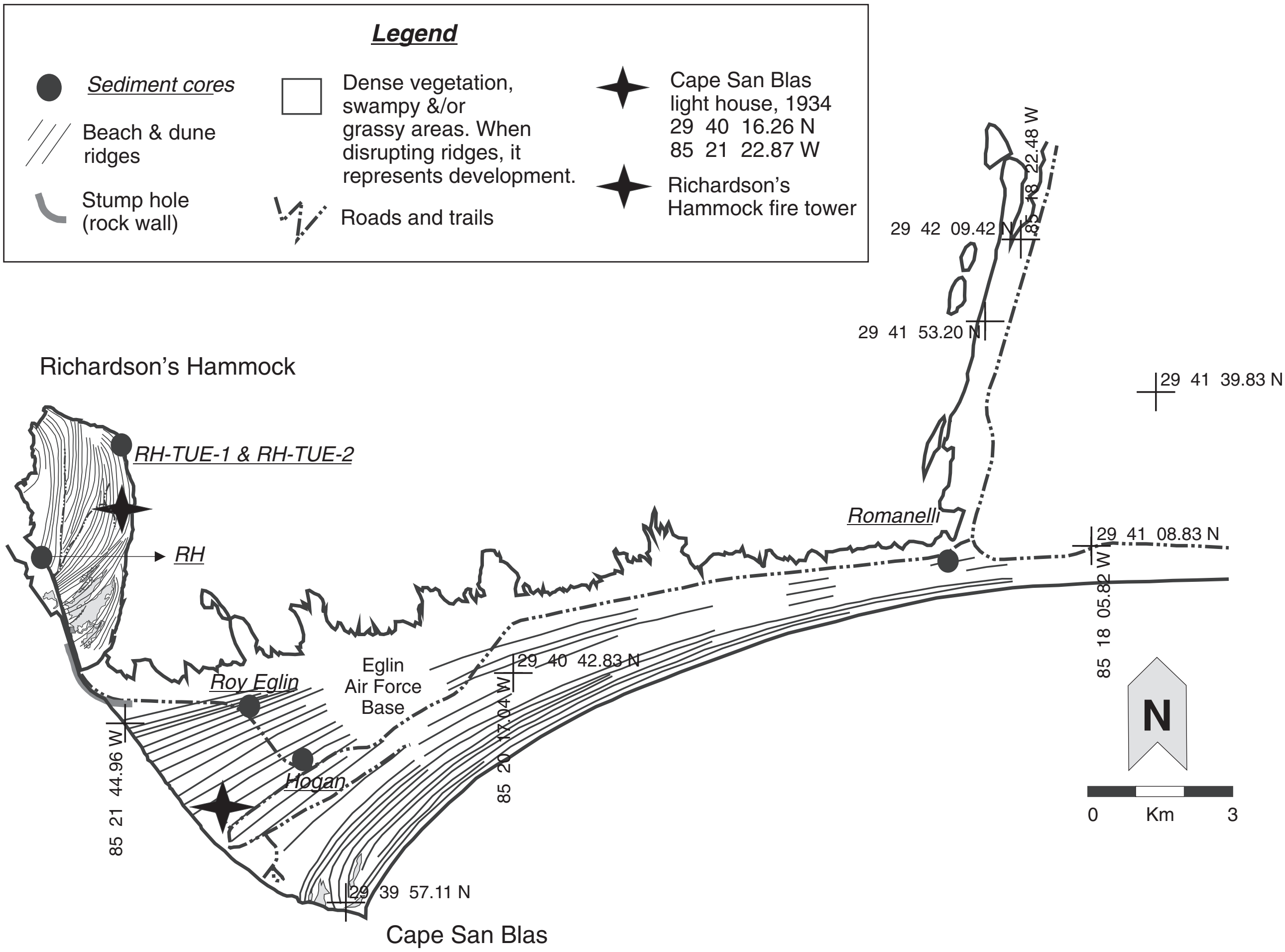

Fig. 3. Map of Cape San Blas and Richardson's Hammock, showing a section of the Lower Mainland. Sediment cores collected within these two systems are shown. For OSL ages of the lowermost sample of each sediment core, please refer to Fig. 2. Ridge patterns and other geomorphological features traced from DOQQ images (USGS, 2004) and topographic/bathymetric 7.5 Minute Series Orthophotomap "Cape San Blas Quadrangle, Florida Gulf CO — 29085-F3-TB-024", USGS (1982). Geographical coordinates are in NAD 83.

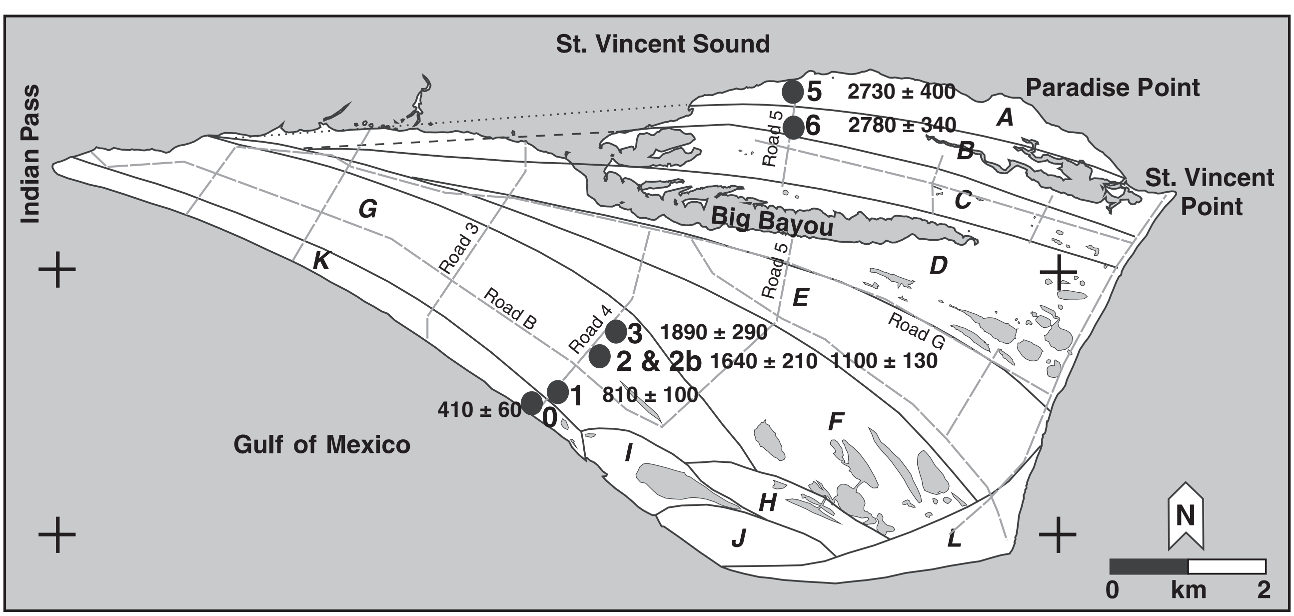

Fig. 4. Map of St. Vincent Island showing the location of the location of the sediment cores collected (as per López and Rink, 2008). OSL ages given (in years before *datum*) correspond to the lowermost sample of each sediment core. The strandplain is divided according to geomorphological ridge sets (from A — oldest to L — youngest) as suggested by Tanner et al. (1989) and Tanner (1992) and discussed in López and Rink (2008). The island has been digitized from DOQQ images (USGS, 1999, 2004) and topographic/bathymetric 7.5 Minute Series Orthophotomaps "Indian Pass Quadrangle, Florida — 29085-F2-TB-024" and "West Pass Quadrangle, Florida Franklin CO — 29085-F1-TB-024", USGS (1982). Geographical coordinates in NAD 83. For symbols refer to the legend in Fig. 3.

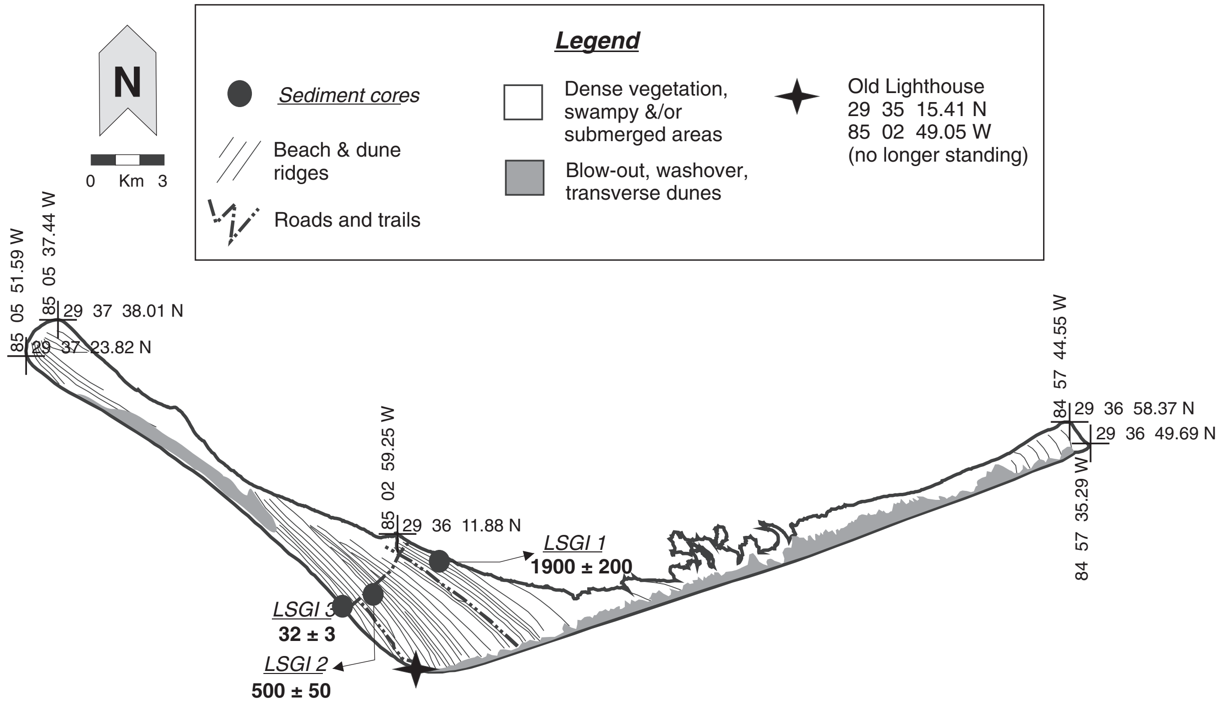

Fig. 5. Geomorphological map of Little St. George Island showing the location of the sediment cores collected. OSL ages given (in years before *datum*) correspond to the lowermost sample of each sediment core. Ridge patterns and other geomorphological features were traced from DOQQ images (USGS, 2004) and topographic/bathymetric 7.5 Minute Series Orthophotomaps "Cape St. George Quadrangle, Florida Franklin CO — 29085-E1-TB-024" (USGS, 1982) and "New Inlet Quadrangle, Florida Franklin CO — N2930-W8452.5/7.5" (USGS, 1981). Geographical coordinates in NAD 83.

Progradation rates were determined by measuring the distance perpendicular to the strike of the ridge set to the shoreline and dividing that by the age difference between the earliest and the latest fully formed ridges. Maximum, minimum and mean rates were determined, in order to give a feel for the uncertainty in the value that arises from uncertainty in the two OSL ages that are involved in each calculation. The statistically derived maximum and minimum ridge accumulations are calculated as follows:

$$\textit{Maximum ridge accumulation rate}(\text{years / ridge})$$
$$= (\textit{max. age of older sample} - \textit{min. age of younger sample}) / \textit{ridge count}$$

$$\textit{Minimum ridge accumulation rate}(\text{years / ridge})$$
$$= (\textit{min. age of older sample} - \textit{max. age of younger sample}) / \textit{ridge count}$$

In general, the calculated rates reflect maximum estimates given that potential gaps may exist in the sedimentary record due to possible hiatuses in sediment accumulation and/or erosive events.

4. Results

Based on five field seasons of work, we have determined the sequence of events related to the emergence of these landforms (López, 2007; López and Rink, 2008). The ages given here are all in absolute years before the time of measurement (i.e. *datum*, in Table 2). Those at the base of each core (samples As) are interpreted as *terminus ante quem* ages (equivalent to the term used by others: minimum-limiting), meaning that these ages are the latest possible ages for land emergence, i.e. the initiation of the beach ridge. We also refer to these as emplacement age estimates. Ages in the upper portions of cores (samples Bs) capture moments in time of aeolian accumulation thereafter, post-dating the initial formation of the ridge. None of the samples reported herein showed conclusive evidence of incomplete zeroing (López, 2007) based on comparisons of histograms of 3 mm vs. 8 mm aliquots (Table 1). The occasional larger equivalent doses found were attributed to beta-dose-related inhomogeneities in the sediments.

With sensitivity to Hesp's (2006) recent redefinition of ridge categories based on mode of origin, we have chose to generally categorize the ridges we have studied in a general geomorphological way (except for the clear foredune ridges we have studied that form category 3 in the following). This is because we feel that we are not able to categorize the ridges (of type 1 and 2 in the following) based on mode of origin (the sedimentological characteristics we can observe in the cores are not sufficient to do this). The various ridges throughout the study area may be divided into three general categories, based on their geometry, height, and geographical position within each barrier system:

Type 1 Relict beach-type ridges located predominantly in the interior and back areas of each barrier, with maximum elevations of 4 m and overtopped with a moderate aeolian cap.

Type 2 Relict dune-type ridges that are relatively close to the open Gulf shoreline, located along the Gulf-side of SJP within its central and north sections. These ridges show elevations exceeding 3–4 m and are decorated with a thick aeolian cap.

Type 3 Foredune ridges.

The type of ridge that was cored in each case is given in Table 5.

Tables 1–3 show details of location, core depth and luminescence data, as well as the OSL results obtained for the samples selected for this study. The samples are part of a major investigation that re-evaluated the supra-tidal evolution of ABIC (López, 2007). The results presented include progradation rates and ASAR previously published for SVI (see López and Rink, 2008).

Fig. 6 shows an example of one of our cores, showing the stratigraphy at core SVI #0. The core is characterized by massive sand in the upper portions, and laminated sand near the base. Some organic material is also

Table 1
Geographical coordinates, coring data and equivalent dose analysis data.

Barrier system and core name	Latitude N[a]	Longitude W[a]	Total core length (cm)	OSL sample	Burial depth of sample (cm)	Aliquot size (mm)	No. of aliquots[b]	D_E (Gy)[c]	D_E error (Gy)[c]
Cape San Blas									
Roy Eglin	29° 40′ 35.95″	85° 21′ 16.15″	331.9	B	90.1	8	23	0.11	<0.01
						3	23	0.11	<0.01
				A	301.6	8	22	0.21	<0.01
						3	24	0.19	<0.01
Hogan	29° 40′ 25.39″	85° 21′ 04.89″	218.0	B	112.2	8	22	0.08	0.01
						3	20	0.07	<0.01
				A	209.8	8	22	0.10	<0.01
						3	20	0.11	0.01
Romanelli	29° 41′ 05.57″	85° 18′ 38.39″	360.2	B	85.0	8	24	0.04	<0.01
						3	16	0.05	0.01
				A	349.2	8	22	0.49	0.02
						3	22	0.49	0.10
Little St. George Island									
LSGI 1	29° 36′ 00.07″	85° 02′ 38.23″	272.8	B	95.9	8	17	0.47	0.03
						1	14	0.48	0.02
				A	214.4	8	24	0.65	0.05
						3	24	0.59	0.05
LSGI 2	29° 35′ 47.11″	85° 03′ 10.87″	222.8	B	84.3	8	22	0.12	0.01
						3	22	0.16	0.06
				A	192.7	8	17	0.14	0.01
						1	12	0.13	0.02
LSGI 3	29° 35′ 41.71″	85° 03′ 22.57″	226.8	B	90.7	8	10	0.01	<0.01
						3	12	0.02	<0.01
				A	158.8	8	17	0.01	<0.01
						1	12	0.02	<0.01

[a] Geographic coordinates are NAD 83.
[b] Number of aliquots accepted for calculation of the equivalent dose after all criteria were met.
[c] D_E is equivalent dose.

present. The positions of samples A and B are also noted. This example is similar to most cores that were extracted.

In general, the OSL ages associated with the samples analyzed in this study are in stratigraphic order within each core, with the exception of the samples in core SVI #6 that are statistically indistinguishable (see Table 1, Fig. 4). All of the OSL ages are in correct temporal sequence, concordant with expectation that ridge progradation proceeded toward the open Gulf of Mexico in all cases (Figs. 1–5; ages for the basal sample A are shown in Figs. 2–5). Fig. 7 shows the relationship between its basal OSL age and geographic position, indicating a clear younging of ridge emplacement towards the Gulf of Mexico. It can also be seen that SJP growth (Fig. 2) has a strong northerly component.

In general, the oldest ridges are located along the shores of St. Joseph Bay, St. Vincent sound (north of SVI) and Apalachicola Bay (north of LSGI — see Fig. 1), while the youngest ridges are currently located within the first 100 m from the Gulf of Mexico shoreline, throughout ABIC. Based on our OSL ages, the oldest barriers of ABIC are Richardson's Hammock (Fig. 2) and SVI (Fig. 4). Sometime during the evolution of SVI, several potential sandy nuclei emerged to the north of Richardson's Hammock and to the east of SVI: the central-north section of LSGI (Fig. 5) and two middle segments of SJP; the area around the Rish Park core and the area just south of Eagle Harbor (Fig. 2). It is hypothesised that barrier progradation took place radiating from these different nuclei in a multi-directional seaward pattern in response to dominant longshore drift and sediment supply, allowing the formation of the different barrier geometries and ridge set patterns currently present throughout ABIC (Fig. 1). The last barrier system to have evolved was most probably CSB, less than about 1000 years ago, forming the nearly enclosed basin currently known as St. Joseph Bay. This would have occurred by seaward growth (both to the west and south) of a tombolo from the mainland to the southern tip of SJP.

Table 2
OSL ages, dose rates and chemical analyses.

Barrier system and core name	OSL sample	^{238}Uranium (ppm)	^{232}Thorium (ppm)	^{40}Potassium (ppm)	Moisture content (wt.%)	Cosmic dose rate (μGy/a)	Annual dose (μGy/a)	SAR-OSL age (year)	*Datum*	Author
Cape San Blas										
Roy Eglin	B	0.17 ± 0.1	0.20 ± 0.04	176 ± 17	14	203	277 ± 15	400 ± 30	2004	López, 2007
	A	0.41 ± 0.1	0.87 ± 0.07	78 ± 15	8	171	336 ± 16	630 ± 40	2004	
Hogan	B	0.18 ± 0.1	0.40 ± 0.10	328 ± 14	18	197	295 ± 15	270 ± 30	2006	López, 2007
	A	0.25 ± 0.1	0.50 ± 0.10	380 ± 17	22	182	301 ± 15	330 ± 20	2006	
Romanelli	B	0.37 ± 0.1	0.90 ± 0.10	357 ± 16	3	205	396 ± 17	100 ± 6	2006	López, 2007
	A	1.53 ± 0.1	5.70 ± 0.40	148 ± 12	4	165	927 ± 26	530 ± 40	2006	
Little St. George Island										
LSGI 1	B	0.16 ± 0.1	0.35 ± 0.05	988 ± 35	19	201	346 ± 15	1400 ± 100	2006	López, 2007
	A	0.25 ± 0.1	0.93 ± 0.08	364 ± 18	3	181	348 ± 17	1900 ± 200	2006	
LSGI 2	B	0.16 ± 0.1	0.52 ± 0.06	222 ± 15	3	206	309 ± 17	390 ± 40	2006	López, 2007
	A	0.16 ± 0.1	0.56 ± 0.06	146 ± 13	8	184	279 ± 16	500 ± 50	2006	
LSGI 3	B	0.36 ± 0.1	1.87 ± 0.14	284 ± 16	5	202	446 ± 18	22 ± 4	2006	López, 2007
	A	0.18 ± 0.1	0.68 ± 0.07	262 ± 16	7	188	307 ± 16	32 ± 3	2006	

Table 3
OSL age data of previously reported samples for St. Joseph Peninsula, Richardson's Hammock and St. Vincent Island (see López, 2007; López and Rink, 2008; Thompson et al., 2007).

Barrier system and core name	OSL sample	Burial depth (cm)	SAR-OSL age (yr)	Author/ publication
St. Joseph Peninsula				
Haven	B	108.9	840 ± 60	López (2007)
	A	249.0	950 ± 80	
Rish Park	B	63.3	1600 ± 100	López (2007)
	A	143.8	2200 ± 200	
White Sands	B	62.4	24 ± 1	López (2007)
	A	249.5	170 ± 10	
Harvey	B	89.5	1300 ± 200	López (2007)
	A	329.5	1700 ± 100	
Old Cedar 1	Horizontal core	50.0	940 ± 110	Thompson et al. (2007)
Deer Ridge SJ201	A	135.1	1000 ± 80	López (2007)
Deer Ridge 1	B	90.6	1300 ± 100	López (2007)
	A	169.8	1500 ± 100	
Deer Ridge 2	A	151.9	1600 ± 100	López (2007)
Wild	B	86.7	690 ± 60	López (2007)
	A	290.8	930 ± 70	
SJ 002 1	B	140.0	140 ± 20	López (2007)
	A	230.9	190 ± 30	
SJ 002 2	B	91.7	110 ± 8	López (2007)
	A	173.9	120 ± 8	
GPR 1	B	99.1	220 ± 40	López (2007)
	A	217.9	250 ± 20	
Richardson's Hammock				
RH-TUE-1	Horizontal core	30.0	1400 ± 100	López (2007)
RH-TUE-2	Horizontal core	190.0	3300 ± 300	López (2007)
RH	B	170.1	2300 ± 200	López (2007)
	A	317.8	3100 ± 300	
St. Vincent Island				
SVI 0	OSL 2	102.4	370 ± 50	López and Rink (2008)
	OSL 1	180.9	410 ± 60	
SVI 1	OSL 2	100.8	710 ± 70	López and Rink (2008)
	OSL 1	167.4	810 ± 100	
SVI 2	OSL 2	99.9	780 ± 100	López and Rink (2008)
	OSL 1	217.1	1640 ± 210	
SVI 2b	OSL 2	98.5	840 ± 100	López and Rink (2008)
	OSL 1	159.6	1100 ± 130	
SVI 3	OSL 2	103.8	920 ± 130	López and Rink (2008)
	OSL 1	246.4	1890 ± 290	
SVI 5	OSL 2	103.6	2860 ± 340	López and Rink (2008)
	OSL 1	222.6	2730 ± 400	
SVI 6	OSL 2	88.9	2790 ± 290	López and Rink (2008)
	OSL 1	156.1	2780 ± 340	

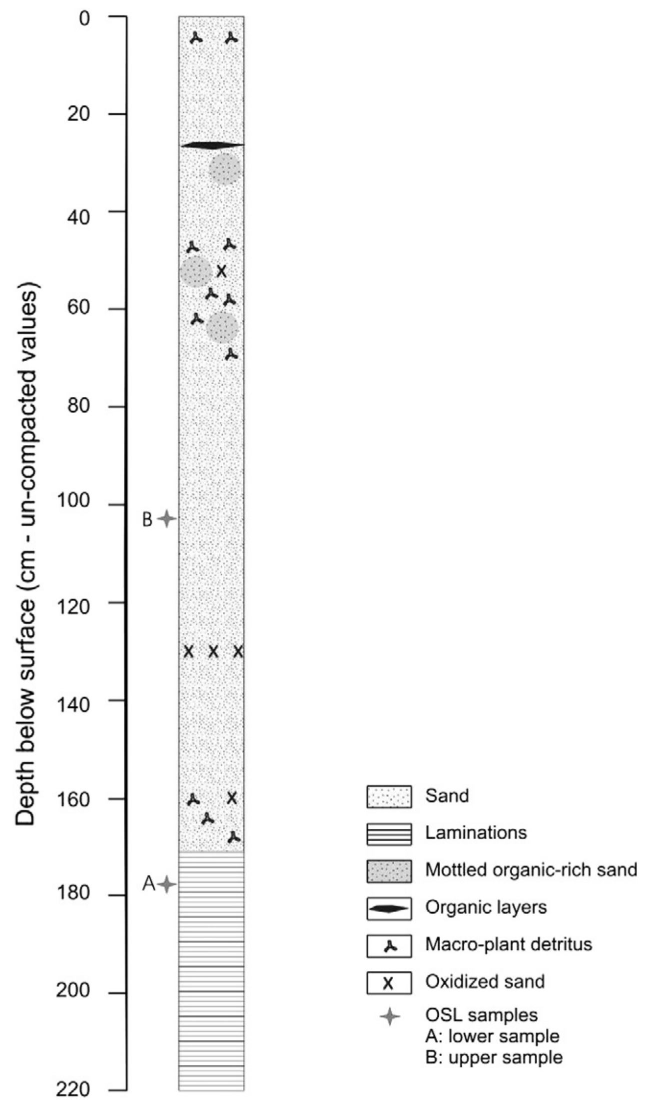

Fig. 6. Example of a sedimentary log showing the stratigraphy of the ridge where sediment core SVI 0 was taken on St. Vincent Island.

4.1. Progradation rates and ridge accretion rates (RAR)

Due to the fact that our basal dated samples (i.e. samples A) do not correspond to the base of each ridge cored, they are indicative of a floating chronology of ridge initiation as these ages mark a *terminus ante quem* for the formation of the ridges (i.e. the basal part of the ridge had to be formed prior to the OSL age we are assigning to sample A). With this in mind, our reported progradation rates are estimates that could only be refined by further coring to the base of the aeolian sequences in each ridge. Nevertheless, the similarities in progradation rates (and ridge accumulation rates (RAR)) within most of the separate areas of the study area attest to the likelihood that they are reflective of the history of progradation.

Table 4 provides the ridge accumulation rates (RAR) and the mean progradation rates for selected sequences in each of the study areas. We found that the progradation rate varies strongly among the different portions of the ABIC, but are generally similar for each portion. On SVI, the calculated progradation rate obtained was 92 m/100 years, and a RAR of one ridge formed every 82 years. On LSGI, the best estimate obtained was of 228 m/100 years; i.e. 89 years/ridge. On CSB it fluctuated considerably depending on the end member selected, however, the best estimate is 527 m/100 years as it was calculated between two known locations (i.e. two core samples) rather than a sample and the coastline as the shoreline in CSB is known to be extremely active (i.e. seasonal erosion/accretion). Hence, the best estimate for CSB is one ridge forming every 38 years. On SJP, the only possible calculations were for the north and south areas of GPR-1 towards the northern end of the peninsula. We see a similar fast progradation rate for Forrest A to GPR (691 m/100 years) to that found at CSB (695 m/100 years). On RH, the estimated progradation rate was 225 m/100 years, and the RAR was 10 years/ridge.

In general, the progradation rates ranged from 92 to 848 m/ 100 years (see Table 4). Beach ridges are relict morphological features (see Tanner, 1995; Taylor and Stone, 1996; Otvos, 2000) and accurate progradation rates are best established between known dated localities. Nevertheless, because foredunes are likely to become relict ridges in our study area, we have also chosen to report progradation rates and RARs for some sequences terminated by foredune ridges.

There are two groups of mean RARs (see Table 4): a) those systems that show an ~80 year average and higher between ridge formation (reaching up to 94 years), and b) those that evolved at less than 40 years per ridge. We only found one case (RH) where there was a

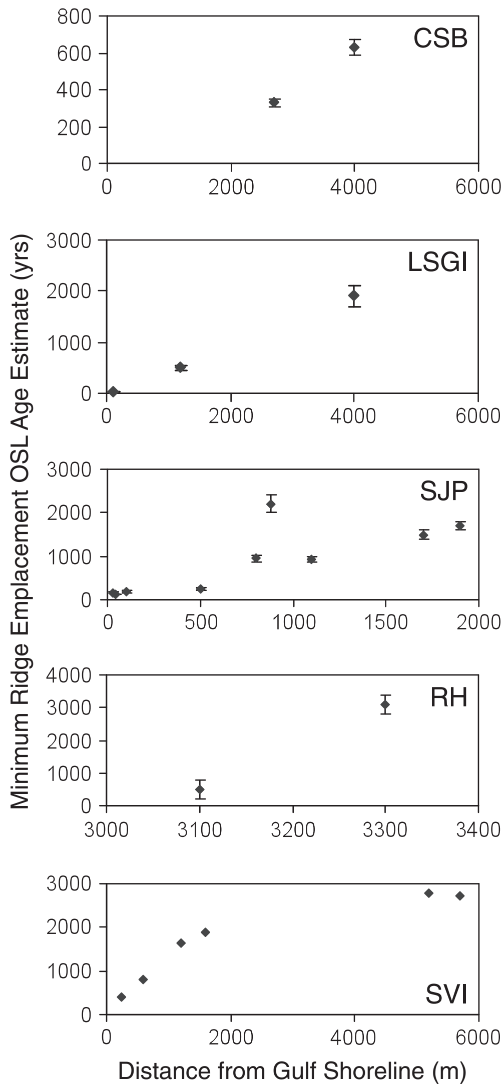

Fig. 7. Diagrams showing the correlation between the lowermost sample OSL age (minimum ridge emplacement age) within selected sediment cores and the distance of the associated sediment core to the Gulf shoreline.

negative age overlap in the calculation of the minimum (RAR), disallowing an estimate of its value (that is, that the minimum age of the older sample was younger than the maximum age of the younger sample).

The slower ridge accumulations (>80 years between ridge formation) occurred in two areas: south-western SVI (Fig. 4), and north-central LSGI (Fig. 5). At LSGI we were able to calculate the RAR by determining the difference between cores LSGI 1, LSGI 2 and LSGI 3. The minimum mean RAR for LSGI was 78 years while the maximum mean obtained was 94 years (see Table 4). At SVI, we found a mean RAR of 82 years between ridge formation, but a maximum/minimum range from 63 to 102 years (López and Rink, 2008). Overall, it seems that the RAR at both locations was similar in magnitude, and both of these landforms are located in the eastern part of the study area backed by Apalachicola Bay (into which the Apalachicola River flows) and St. Vincent Sound.

The faster progradation rates (i.e. lower RARs) were found in three areas; all around St. Joseph Bay (see Fig. 1): RH, central northern SJP and CSB. At RH, despite the fact that the mean ages at either end overlap in uncertainty, a sequence of 20 ridges was constrained by an emergence age at either end, yielding an estimate of 10 to 40 years per ridge (depending upon whether the max age range vs. the mean age range was used). A rate of 38 years between ridge formations was found for the north-western interior portion of CSB between the Roy Eglin and Hogan coring locations (see Fig. 3).

Taken as a whole, we find more rapid lateral progradation in the beach ridge sequences fronting St. Joseph Bay, in the western section of the study area, but rather slower lateral progradation rates for those in front of Apalachicola Bay (at LSGI) and for those in front of St. Vincent Sound (at SVI) (see Fig. 1). Beach ridge emplacement age estimates are plotted against distance from the Gulf Shoreline in Fig. 7. This shows the expected relationship between geomorphic age of the ridges and geographical position, but is quantified through the valuable tool of OSL.

For one case at CSB (Hogan to Gulf-shore) and the case of GPR-1 to the modern shoreline on northern SJP, the modern shoreline foredune was used as an endpoint in the progradation rate calculation. These differ from the other cases where actual dated endpoints are given by ridge emplacement age estimates. We acknowledge that all of the progradation rates and ridge accumulation rates are simply estimates of the average rates: these estimates do not take into account the effects on the true rate of progradation that might be different if erosional periods occurred during the intervals or if variations in directionality and/or sediment supply occurred through time.

4.2. Average sediment accumulation rates (ASAR)

A compilation of ASAR for 24 individual locations throughout the study area of the ABIC is given in Table 5. ASAR values reported herein span decadal to millennial time scales: the difference in the OSL ages between the lower and upper samples within the same sediment core (or stratigraphic profile) is as little as 10 years (cores SJ 002 1 and LSGI 3) or as large as 970 years (core SVI #3). However, similar and longer intervals came from stratigraphic profiles associated with archaeological sites, where the anthropogenic layer was in between the OSL-dated layers: 940 years for the Old Cedar 1 and 1900 years for Richardson's Hammock TUE, both coastal shell-midden sites (see López, 2007 and Thompson et al., 2007).

The Lower ASAR values, which correspond to early stages of aeolian growth at the selected ridge locations, were seen to fall into two groups: a) those showing accumulations of less than 1.7 cm/year (18 locations out of 21 = 86%) and b) those in the range of 2 to 8 cm/year (3 locations out of 21 = 14%). The great majority of sediment cores fell into the first category and had a range of 0.08 to 1.96 cm/year (see Table 5), whereas only three fell into the second category and they had a range of 3.96 to 8.22 cm/year. A significant proportion (60%) of those cores from within 200 m of the Gulf Shoreline had Lower ASAR's of > 1.7 cm/year (LSGI 3, SJ002 1 and SJ002 2). All of these ridges belong either to Type 2 or Type 3 ridges.

For the Upper ASAR, which corresponded to the later stages of aeolian growth at each ridge location, most sediment cores (19 locations out of 23 = 83%) had values of less than 0.5 cm/year, with the remainder yielding values that ranged from 0.83 to 4.12 cm/year (4 locations out of 23 = 14%). The latter 4 ridges all belong to Type 2 and 3 ridges, while the former group of 19 belong to Type 1 ridges.

We considered how the sedimentation rates for the Lower ASAR were distributed with respect to distance to the open Gulf Shoreline (Fig. 8): all show a strong decreasing Lower ASAR with distance from the coast. This dependence indicates that a lower accumulation rate had occurred as the location was stranded further inland as new ridges were formed seaward of it. This trend continues in all the study areas for the Upper ASAR (Fig. 8), which represents the aeolian sediment accumulation at even later times, when the ridges are even further away from the open Gulf of Mexico.

The highest ASAR values at deep inland locations occur at CSB, in both the Upper and Lower ASAR's (see Fig. 8). These ridges range from about 300 to 600 years old and lie at distances of 2700 to 4000 m from the open Gulf. Comparison of Upper and Lower ASAR at individual locations clearly shows that more rapid aeolian accumulation occurs in the early life of a new beach ridge, followed by a slowing of this accumulation rate.

To amplify our observation that sedimentation rates diminish over time in the early stages of inland stranding of sandy ridges, we provide a

Table 4
Ridge accumulation rates (RAR) and progradation rates.

Barrier system and figure #	Core names at extremities of ridge set	Ridge total[a]	Age range (years) Max range Min range[b]	Min Max Ridge accum. rate (years/ridge)[c]	Mean ridge accum. rate (years/ridge)[c]	Prograd. rate (m/years)[d]	Prograd. rate (m/100 years)
St. Vincent Island							
4	SVI 3–SVI 0	18	2180–350	102	82	1300 m/1482 years	92
			1600–470	63			
Little St. George Island							
5	LSGI 1–LSGI 2	15	2100–450	110	94	3050 m/1400 years	218
			1700–550	77			
5	LSGI 2–LSGI 3	6	550–29	87	78	1200 m/468 years	256
			450–35	69			
5	LSGI 1–LSGI 3	21	2100–29	99	89	4250 m/1868 years	228
			1700–35	79			
Cape San Blas							
6	RE–HOG	8	670–310	45	38	1580 m/300 years	527
			590–350	30			
6	HOG–Gulf shore	15	350–0	23	22	2800 m/330 years	848
			310–0	21			
6	RE–Gulf shore	23	670–0	29	28	4380 m/630 years	695
			590–0	26			
St. Joseph Peninsula							
2	GPR 1 — End of Spit	7	270–0	39	36	615 m/250 years	246
			230–0	33			
2	Forrest A — GPR 1	17	650–230	25	21	2419 m/350 years	691
			550–270	17			
Richardson Hammock							
3	RH TUE 2 — RH	20	3600–2800	40	10	450 m/200 years	225
			Stat. Indisting.	NA			

[a] As determined from topographic maps and DOQQ images of the different barrier systems.
[b] Calculated as follows: maximum range = age + error minimum range = age − error.
[c] Calculated as follows: minimum ridge accumulation rate = (minimum age of older sample − maximum age of younger sample)/ridge count; maximum ridge accumulation rate = (maximum age of older sample − minimum age of younger sample)/ridge count.
[d] Based on the distance between the two cores being compared or the core and the shoreline.

subset of our results in Table 6, which all have *terminus ante quem* ages between 250 and 630 years ago, and are separated from the Gulf shoreline by other ridges. For this group of young ridges it is clear that the Upper ASAR is always lower than its corresponding Lower ASAR. Moreover, we also observe that the Upper ASAR is less variable than the Lower ASAR. The standard deviation among the five Upper ASARs is only 31% of the mean, while the same value for the Lower ASAR is 59%. This fits with the idea that local onshore conditions (associated with factors such as wind direction, beach geometry and sand supply) are more highly variable among the five locations, than the conditions which control aeolian accumulation experienced by the ridges after they are stranded inland.

We observe that the very lowest Upper ASAR values occur in two types of locations: a) the oldest beach ridges located on the back of the barrier islands, and b) on now protected bay-side locations with archaeological middens. Examples of the first case are the two oldest ridges dated on SVI, cores SVI 5 and 6, which had Upper ASAR values of 0.04 and 0.03 cm/year respectively. In the second case the locations are at Old Cedar and Richardson's Hammock TUE midden sites, where the Upper ASAR values were 0.03 and 0.02 cm/year respectively. Both of the latter were covered by high-canopy old-growth oak groves, which may in part have been originally established by high levels of nutrients that were introduced anthropogenically. It is possible that these high canopies reduced wind velocities greatly reducing penetration of aeolian sediment across the land surface over long periods of time.

5. Discussion

5.1. Progradation rates and RAR

We can compare our results shown in Table 4 to other studies of rates of progradation of ridge sequences. Murray-Wallace et al. (2002) used OSL to determine the time of formation of a number of dune ridges that evolved over the last 4000 years within Guichen Bay in South Australia. They found a RAR of 80 years between consecutive ridges which is similar to our mean RARs of 94 years for LSGI. In addition, their rate is virtually identical to the SVI segment of 82 years per ridge (see Table 4 and López and Rink, 2008). Murray-Wallace et al. (2002) reported a progradation rate for the same sequence of 39 m/100 years, which is about 50% slower than the SVI sequence and much slower than all of our other progradation rates.

Closer to our study area, but on Florida's east coast at Cape Canaveral, Rink and Forrest (2005) used OSL to determine the ages of an extensive sequence of about 50 ridges that grew over the last 3700 years. The average RAR was 80 ± 8 years/ridge with a mean progradation rate of 135 ± 12 m/100 years. Again, the Canaveral RAR is comparable to both the SVI and Guichen Bay ridge sequences, though at Canaveral only ridges on topographic maps enclosed by 3 m-contour lines were included in ridge counts. The mean progradation rate at Canaveral is slightly larger than at SVI, but considerably smaller than our other smallest progradation rates on two landforms: 218 m/100 years on LSGI and 527 m/100 years on CSB.

All of our progradation rates were faster than those found for a variety of environments along the south-eastern coast of Australia, which ranged from 24 to 57 m/100 years (Thom et al., 1978; Chapman et al., 1982).

Argylan et al. (2005) OSL-dated littoral and aeolian sediments from various Great Lakes well-preserved strandplains in North America, spanning the past 4500 years. The results obtained for three major ridge sequences on bays perched along the shores of Lake Michigan and Lake Superior show ages from < 100 to ~4300 years ago. They report average beach ridge formation rates between 28 ± 3 and 50 ± 4 years for ridges formed prior to ~1500 years ago. For those beach ridges formed within the last ~1500 years, the rates of ridge formation are higher with values

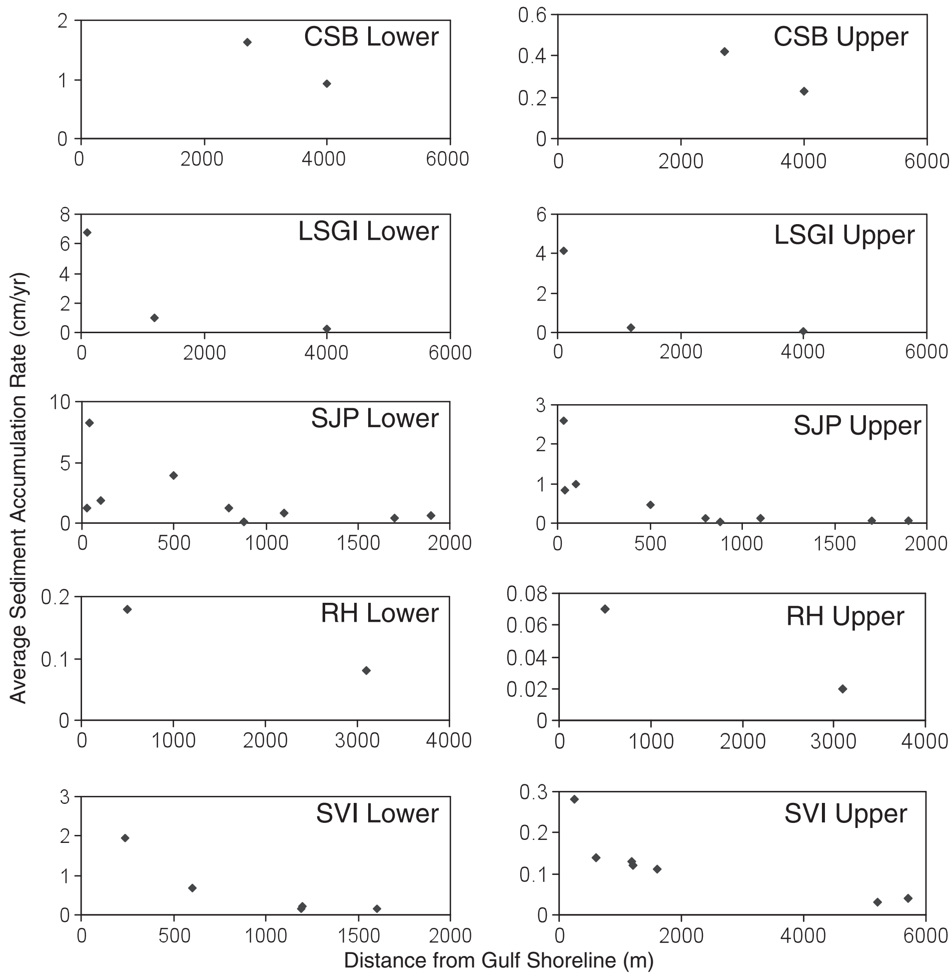

Fig. 8. Diagrams showing the correlation between Average Sediment Accumulation Rates (ASAR) for selected sediment cores and the distance of the associated sediment cores to the Gulf shoreline. Lower ASAR values correspond to the calculation between the Lowermost OSL sample and the Uppermost OSL sample, within each selected sediment core. Upper ASAR values correspond to the calculation between the Uppermost OSL sample and the ground surface, at each selected coring location.

between 62 ± 4 and 137 ± 7 years. Interestingly, we find the opposite: longer intervals between ridge formation (>80 years/ridge) occurred in our older intervals (>~1000 years ago) and shorter intervals between ridges (<40 years/ridge) for our younger segments (<700 years ago) throughout the ABIC.

5.2. Average sediment accumulation rates (ASAR)

The most notable aspect of the relationship between ASAR and the distance to the current Gulf of Mexico Shoreline is that aeolian accumulation does not drop to zero as ridges are stranded inland (see Table 5). Rather, aeolian sediment accumulation continued well after the ridge was formed, and undoubtedly in many cases, well after it became vegetated. This was first reported for SVI by the authors in López and Rink (2008). We see the same trend for these other areas reported herein. Possible explanations for this continuing aeolian sedimentation as the ridges are stranded inland away from sediment supply are: a) large storms that may move sand inland under high wind velocities, and b) the effects of major fires that can reduce the size of the vegetation cover, thus allowing better penetration of aeolian sediment across the surfaces of these areas.

We observe highly variable Lower ASARs that may correspond, in depositional time, to the early stages of aeolian deposition. However, it has been noted that sediment accumulation rates are a reflection of the beach ridge dimension in general: low rates are associated with large beach ridges whereas high rates are correspondent to small ones (c.f. Taylor and Stone, 1996). Consider only the ridges we studied within 100 m of the present shoreline; these occur at SJP (White Sands, SJ 002 1 and SJ 002 2) and on LSGI (LSGI 3). These four sites are all Type 2 or Type 3. For these we observe Lower ASARs ranging from to 1.28 to 8.22 cm/year for locations ranging in emplacement age from 32 ± 3 to 190 ± 30 years ago at distances from 30 to 100 m from the present Gulf shoreline. The mean value of Lower ASAR for these four examples is 4.53 ± 3.02 cm/year. It is not unexpected to see such a large range of ASAR values during the initial interval of growth of a ridge due to the variation in formational factors such as local nearshore geometry, foreshore and back-beach geometry and sand supply, among other external factors.

We are not aware of any published local studies of aeolian sediment accumulation rates, though we are able to compare our ASAR values with those of only two other studies. McLean and Shen (2006) who conducted a 30-year-long study of dune growth following a large storm at Moruya Beach in south-eastern Australia. Table 7 shows a compilation of their ASAR results from four locations along the beach. Though their mean value of 8.4 ± 2.3 cm/year is higher than our Lower ASAR mean for our youngest ridges of 4.53 ± 3.02 cm/year (i.e. White Sands, SJ 002 1, SJ 002 2, and LSGI 3), it is statistically indistinguishable from it. Notwithstanding, all the differences that must exist between the two beach systems, the OSL-derived results seem to be reasonable in comparison with this study. In another coastal dune formation study along the central-western shores of Denmark, Aagaard et al. (2007) conducted a high resolution composite study of a complex dune field involving historical shoreline maps, ground penetrating radar, detailed stratigraphy and OSL-dating. They report that over the past 300 years, the mean vertical accretion rates at two of the cored sites are 13 and 18 cm/year., in dunes

Table 5
Average sediment accumulation rates (ASAR) and distances of cores from Gulf Shoreline.

Barrier system and core name	Ridge type	Distance from gulf shoreline (m)	Lower ASAR[a] (cm/year)	Upper ASAR[a] (cm/year)
Cape San Blas				
Roy Eglin	1	4000	0.92	0.23
Hogan	1	2700	1.63	0.42
Little St. George Island				
LSGI 1	1	4000	0.24	0.07
LSGI 2	1	1200	0.99	0.22
LSGI 3	3	100	6.80	4.12
St. Joseph Peninsula				
Haven	1	800	1.27[b]	0.13
Rish Park	1	880	0.13	0.04
White Sands	3	30	1.28	2.6
Harvey	1	1900	0.6	0.07
Deer Ridge 1	1	1700	0.40	0.07
Wild	1	1100	0.85	0.13
SJ 002 1	2	100	1.82	1.00
SJ 002 2	3	40	8.22[b]	0.83
GPR 1	1	500	3.96	0.45
Richardson's Hammock				
RH-TUE-1	1	3100	0.08[c]	0.02
RH	1	500	0.18	0.07
St. Vincent Island				
SVI 0	1	240	1.96[b]	0.28
SVI 1	1	600	0.67	0.14
SVI 2	1	1190	0.14	0.13
SVI 2b	1	1200	0.23	0.12
SVI 3	1	1600	0.15	0.11
SVI 5	1	5700	n/a[d]	0.04
SVI 6	1	5200	n/a[d]	0.03

[a] ASAR is average sediment accumulation rate.
[b] Minimum values since ages in calculation overlap within uncertainty.
[c] Used age of lower horizontal core RH-TUE-2 for time control.
[d] Not available because ages in the corresponding interval are stratigraphically reversed and indistinguishable.

with elevations more than 8 m high. These values are much higher than any of our ASAR values. However, the active dune fields studied by Aagaard et al. (2007) extend for ~500 m inland and are openly exposed to the North Sea on the south-eastern tip of Skallingen Spit. Little to no low-lying vegetation is present and the authors associate sediment supply with overwash, surge and onshore sediment control.

6. Conclusions

The use of coring on beach ridge crests has allowed the use of OSL ages for the determination of vertical accumulation rates of sediments (average sediment accumulation rates: ASARs) by direct dating of multiple samples within individual sediment cores. In addition, estimates of ridge accumulation rates (RARs) and lateral progradation rates were also made by comparison of basal ages in cores at positions along transects (perpendicular to the current shoreline) that strike across ridge sequences containing multiple relict sandy ridges. The ASAR results were shown to be plausible through comparison with direct survey of beach profiles by other authors documenting active sediment accumulation over a 30-year period. Our results demonstrate that up to approximately one order of magnitude lower sedimentation rates occur after an initial period of more rapid aeolian accumulation for the vertical intervals studied in foredune ridges. The progradation rates and ridge accumulation rates (RARs) are in some cases comparable to others found in different parts of the world, and in a number of cases are much faster than previously documented using OSL.

The resolution of the OSL method and this geographical scale of the study area allowed us to identify coastal barrier sections where very rapid accretion of ridges occurred relative to areas of more steady and slower accretion. We were also able to show that CSB probably grew out as a tombolo from the mainland to the base of SJP at a relatively late stage in the history of the area (as late as about 600 years ago, but almost certainly less than about 1000 years ago). We also confirm Stapor's (1973, 1975) early supposition that Richardson's Hammock is the one of the oldest land-forms in the CSB/SJP complex, and that it preceded the formation of St. Joseph Peninsula.

Perhaps our most important finding is that aeolian accumulation does not drop to zero after ridges are stranded landward. This confirms the results of an earlier study by the authors (see López and Rink, 2008) at SVI. By comparing the accumulation rates in very young ridges (100–200 years old) with those stranded inland, ranging from 300 to 600 years old, we established that slowing of the accumulation rate by about one order of magnitude occurs very soon after the ridges are stranded landward. That continuing aeolian sedimentation occurs on ridges well after stranding inland by newer ridges growing seaward is important to considerations of conservation of stranded sequences from the point of view of developers and public stakeholders. This importance is related to considerations among stakeholders regarding how to protect newly constructed infrastructure or to retain existing infrastructure: one can expect it is more likely for it to survive if it either exists or is built on lands that are both old and growing vertically, even if in small increments. Moreover, establishing the rates of vertical sediment accumulation on natural shorelines provides a baseline for understanding the re-growth rates of storm-affected beach and dune ridge complexes.

Table 6
Comparison of ASAR values for a group of young ridges.

Sample	Emplacement age estimate (year)	Lower ASAR (cm/year)	Upper ASAR (cm/year)	No. of ridges away from gulf shoreline
SVI 0	410 ± 60	>1.96	0.28	1
LSGI 2	500 ± 50	0.99	0.22	6
Roy Eglin	630 ± 40	0.92	0.23	23
Hogan	330 ± 20	1.63	0.42	15
GPR 1	250 ± 20	3.96	0.45	5
Mean		1.89 ± 1.11 (59%)	0.32 ± 0.10 (31%)	

Acknowledgements

This research was made possible thanks to logistic, financial and staff support of the T.H. Stone Memorial St. Joseph Peninsula State Park (Florida Department of Environmental Protection) and the Apalachicola National Estuarine Research Reserve, as well as the Saint Vincent Island National Wildlife Refuge (U.S. Department of the Interior). We also acknowledge the exploratory, sampling and coring permissions that were granted by the former entities as well as the Wm. J. Rish Recreation Park (on St. Joseph Peninsula). Financial support was provided through a Natural Science and Engineering Research Council of Canada (NSERC) grant to WJR. We extend our thanks for field assistance during the various field seasons, from 2002 to 2005, to Dr. J. Boyce, J. Etherington, K. Keizars, J. Pilarczyk, K. Moretton, M. Kossak, J. Thompson, and S. Collins (all from McMaster University). We also acknowledge the hospitality of both the Florida State University Coastal and Marine Laboratory for

Table 7
Ridge data from McLean and Shen (2006).

Profile	Accumulation (cm)	Interval (years)	ASAR (cm/year)
1	259	33.92	11.9
2	216	32.08	6.7
3	189	32.08	5.9
4	290	32.08	9.0
Mean			8.4 ± 2.3

WJR's sabbatical visit in 2009 and the Apalachicola National Estuarine Research Reserve for WJR's sabbatical visit in 2004.

References

Aagaard, T., Orford, J., Murray, A.S., 2007. Environmental controls on coastal dune formation: Skallingen Spit, Denmark. Geomorphology 83, 29–47.

Argylan, E.P., Forman, S.L., Johnston, J.W., Wilcox, D.A., 2005. Optically stimulated luminescence dating of late Holocene raised strandplain sequences adjacent to Lakes Michigan and Superior, Upper Peninsula, Michigan, USA. Quaternary Research 63, 122–135.

Ballarini, M., Wallinga, J., Murray, A.S., van Heteren, S., Oost, A.P., Bos, A.J.J., 2003. Optical dating of young coastal dunes on a decadal time scale. Quaternary Science Reviews 22, 1011–1017.

Banerjee, D., Hildebrand, A.N., Murray-Wallace, C.V., Bourman, R.P., Brooke, B.P., Blair, M., 2003. New quartz SAR-OSL ages from the stranded beach dune sequence in south-east South Australia. Quaternary Science Reviews 22, 1019–1025.

Bird, E.C.F., 1976. Coasts. Australian National University Press, Canberra. 282 pp.

Chapman, D.M., Geary, M., Roy, P.S., Thom, B.G., 1982. Coastal Evolution and Coastal Erosion in New South Wales. Coastal Council of New South Wales, Sydney. 341 pp.

Clifton, H.E., Hunter, R., 1982. Coastal sedimentary facies. In: Schwartz, M.L. (Ed.), The Encyclopedia of Beaches and Coastal Environments. Hutchinson Ross Publishing, Stroudbsburg, Pennsylvania, pp. 314–322.

Davies, J.L., 1957. The importance of cut and fill in the development of sand beach ridges. Australian Journal of Science 20, 105–111.

Forrest, B.M., 2003. Applications of luminescence techniques to coastal studies, St. Joseph Peninsula, Gulf County, Florida. Unpublished M.Sc. Thesis, McMaster University, Hamilton, 209 pp.

Hesp, P., 1984. Foredune formation in Southeast Australia. In: Thom, B.G. (Ed.), Coastal Geomorphology in Australia. Academic Press, Sydney, pp. 69–97.

Hesp, P.A., 1999. The beach backshore and beyond. In: Short, A.D. (Ed.), Handbook of Beach and Shoreface Morphodynamics. John Wiley and Sons, New York, pp. 145–169.

Hesp, P., 2002. Foredunes and blowouts: initiation, geomorphology and dynamics. Geomorphology 48, 245–268.

Hesp, P.A., 2006. Sand beach ridges: definitions and re-definition. Journal of Coastal Research Special Issue 39, 72–75.

López, G.I., 2007. The Late Quaternary evolution of the Apalachicola Barrier Island Complex, North-East Gulf of Mexico, as determined from optical dating. Ph.D. Dissertation, School of Geography and Earth Sciences, McMaster University, Hamilton, Canada, 264 pp. (available at: http://www.aber.ac.uk/ancient-tl/).

López, G.I., Rink, W.J., 2008. New Quartz-OSL ages for beach ridges on the St. Vincent Island Holocene Strandplain, Florida, U.S.A. Journal of Coastal Research 24, 49–62.

McLean, R., Shen, J.-S., 2006. From foreshore to foredune: foredune development over the last 30 years at Moruya Beach, New South Wales, Australia. Journal of Coastal Research 22, 28–36.

Miller, J.J., Griffin, J.W., Fryman, M.L., Stapor, F.W., 1981. Archeological and historical survey of St. Vincent National Wildlife Refuge, Florida. Tallahassee, Florida: U.S. Fish and Wildlife Service, Contract A-5831(79), 101p.

Murray, A.S., Wintle, A.G., 2000. Luminescence dating of quartz using an improved single-aliquot regenerative-dose procedure. Radiation Measurements 32, 57–73.

Murray-Wallace, C.V., Banerjee, D., Bourman, R.P., Olley, J.M., Brooke, B.P., 2002. Optically stimulated luminescence dating of Holocene relict foredunes, Guichen Bay, South Australia. Quaternary Science Reviews 21, 1077–1086.

Otvos, E.G., 1992. Apalachicola coast Quaternary evolution, NE Gulf of Mexico. In: Cletcher, C.H., Wehmiller, J.F. (Eds.), Quaternary Coasts of the United States: Marine and Lacustrine Systems. Society of Economic Paleontologists and Mineralogists, Tulsa, pp. 221–232.

Otvos, E.G., 2000. Beach ridges — definitions and significance. Geomorphology 32, 83–108.

Otvos, E.G., 2005. Coastal barriers, Gulf of Mexico: Holocene evolution and chronology. Journal of Coastal Research, Special Issue 42, 141–163.

Rink, W.J., 2003. Thermoluminescence of quartz and feldspar sand grains as a tracer of nearshore environmental prcoesses in the Southeastern Mediterranean Sea. Journal of Coastal Research 19, 723–730.

Rink, W.J., Forrest, B., 2005. Dating evidence for the accretion history of beach ridges on Cape Canaveral and Merritt Island, Florida, USA. Journal of Coastal Research 21, 1000–1009.

Rink, W.J., Pieper, K.D., 2001. Quartz thermoluminescence in a storm deposit and a welded beach ridge. Quaternary Science Reviews 20, 815–820.

Rizk, F.F., 1991. The Late Holocene Development of St. Joseph Spit. Florida State University, Tallahassee.

Roy, P.S., 1991. Shell hash dating and mixing models for palimpsest marine sediments. Radiocarbon 33, 283–289.

Roy, P.S., Cowell, P.J., Ferland, M.A., Thom, B.G., 1994. Wave-dominated coasts. In: Carter, R.W.G., Woodroffe, C.D. (Eds.), Coastal Evolution: Late Quaternary Shoreline Dynamics. Cambridge University Press, Cambridge, pp. 121–186.

Stapor, F.W., 1973. Coastal Sand Budgets and Holocene Beach Ridge Plain Development — Northwest Florida. Florida State University, Tallahassee. 221 pp.

Stapor, F.W., 1975. Holocene beach ridge plain development, Northwest Florida. Zeitschrift für Geomorphologie 22, 116–144.

Stapor, F.W., Tanner, W.F., 1977. Late Holocene mean sea level data from St. Vincent Island and the shape of the Late Holocene mean sea level curve. In: Tanner, W.F. (Ed.), Coastal Sedimentology. Florida State University, Tallahassee, Florida, pp. 35–68.

Tanner, W.F., 1961. Offshore shoals in area of energy deficit. Journal of Sedimentary Petrology 31, 87–95.

Tanner, W.F., 1992. Three thousand years of sea level change. Bulletin American Meteorological Society 73, 297–303.

Tanner, W.F., 1995. Origin of beach ridges and swales. Marine Geology 129, 149–161.

Tanner, W.F., Demirpolate, S., Stapor, F.W., Alvarez, L., 1989. The Gulf of Mexico Late Holocene sea level curve. Transactions Gulf Coast Association of Geological Societies 39, 553–562.

Taylor, M., Stone, G.W., 1996. Beach-ridges: a review. Journal of Coastal Research 12, 612–621.

Thom, B.G., Polach, H.A., Bowman, G.M., 1978. Holocene age structure of coastal sand barriers in New South Wales, Australia. Geography Department Report. Duntroon, University of New South Wales, Canberra. 86 pp.

Thompson, J., Rink, W.J., López, G.I., 2007. Optically stimulated luminescence age of the Old Cedar Midden, St. Joseph Peninsula State Park, Florida. Quaternary Geochronology 2, 350–355.

USGS, 1981. Orthophotomap 7.5 minute series. New Inlet, Florida. N2930-W8452.5/7.5'.

USGS, 1982. Orthophotomaps 7.5 minute series: Indian Pass, Florida 29085-F2-TB-024; St. Joseph Point, Florida 29085-G4-TB-024; St. Joseph Peninsula, Florida 29084-F4-TB-024; Cape San Blas, Florida 29085-F3-TB-024; Cape St. George, Florida 29085-E1-TB-024.

USGS, 1999. Digital Orthographic Quarter-Quads Q4642 and Q4641; Indian Pass — West Pass, Florida; 1 m resolution; UTM projection, NAD 83; 8 quarter-quads. FDEP.

USGS, 2004. Northwest Florida Water Management District (NWFWMD) ADS40 Digital Imagery Acquisition and Natural Color and Color Infrared Orthophoto Production (remote-sensing images). FDEP.